

DEVELOPMENT AND APPLICATIONS OF LASER-INDUCED INCANDESCENCE

Randy L. Vander Wal and Daniel L. Dietrich
 (Nyma Inc.) (NASA-Lewis)
 @ NASA-Lewis
 Cleveland, Ohio

and

Zhiquang Zhou and Mun Y. Choi
 University of Illinois at Chicago
 Chicago, Illinois

Introduction

Presently, several NASA-funded investigations currently focus on soot processes and radiative influences of soot in diffusion flames given their simplicity, practical significance and potential for theoretical modelling. Among the physical parameters characterizing soot, soot volume fraction, f_v , a function of particle size and number density, is often of chief practical interest in these investigations, as this is the geometrical property that directly impacts radiative characteristics and the temperature field of the flame and is basic to understanding soot growth and oxidation processes. Diffusion flames, however, present a number of challenges to the determination of f_v via traditional extinction measurements.

Soot in diffusion flames is often confined to narrow spatial regions with steep concentration gradients limiting the accuracy of inversion methods based on single line-of-sight extinction measurements. Additionally, such inversion techniques have only been demonstrated for axisymmetric systems. An absorption measurement requires a known path length, often made by visualization of the flame, which is imprecise and presents a difficulty for dim flames. In turbulent flames and droplet combustion, both the small spatial scales and time-varying processes have impeded 'instantaneous' measurement of f_v in these systems. Scattering contributions to an extinction measurement are difficult to account for, particularly for time-varying systems and large soot aggregates, hence are often neglected leading to overestimation of the inferred f_v .

By comparison, laser-induced incandescence (LII) possesses several advantages compared to line-of-sight extinction techniques for determination of f_v . Since LII is not a line-of-sight technique, similar to fluorescence, it possesses geometric versatility allowing spatially resolved measurements of f_v in real time in nonaxisymmetric systems without using deconvolution techniques. The spatial resolution of LII is determined by the detector and imaging magnification used. Neither absorption by polycyclic aromatic hydrocarbons (PAH's) nor scattering contributes to the signal. Temporal capabilities are limited only by the laser pulse and camera gate duration, with measurements having been demonstrated with 10 ns resolution. Because of these advantages, LII should be applicable to a variety of combustion processes involving both homogeneous and heterogeneous phases. Our work has focussed on characterization of the technique as well as exploration of its capabilities and is briefly described here.

Description of LII

Laser-induced incandescence uses a pulsed high energy laser to heat soot to incandescent temperatures. For 8-10 nsec. laser pulses, energy balance equations indicate that the energy addition rate greatly exceeds the loss rate

from thermal conduction and radiation[1-5]. For example, the temperature of a soot particle is predicted to rapidly rise to the vaporization temperature of carbon, roughly 4300 K, for laser intensities of 1×10^7 W/cm² or greater. Calculations by Eckbreth[1] show that equilibration of the absorbed energy within the particle occurs rapidly, on the time scale of the laser pulse, but heating of the medium surrounding the particle occurs on a longer time scale. In accord with the Planck radiation law, the particle thermal emission at these elevated temperatures increases and shifts to the blue compared to the non-laser-heated soot and flame gases. Theoretical analysis predicts the LII signal to be nearly proportional to soot volume fraction.[2-5] Qualitatively, large and small LII signals represent high and low soot volume fractions, respectively. Several recent applications of LII involve gas-jet diffusion flames[6-9], premixed flames[6], both fiber-supported and freely falling droplet combustion[10-12] and engine research[13-14].

Figure 1 is a general experimental schematic of our experiments using LII. Major equipment items are the pulsed laser, flame system and detection system. Pulsed laser light from a Nd:YAG laser at either 1064 or 532 nm heats the soot to incandescence temperatures. 'Point' and one-dimensional measurements are performed by aperturing the beam while a laser sheet is formed to obtain two dimensional LII images. For 'point' measurements, various lenses and/or mirrors direct the incandescence signal into a monochromator with a photomultiplier as detector. A gated intensified array camera preceded by various filters and a UV lens often fitted with an extension tube is used to obtain LII images. LII images are captured digitally using a frame-grabber with 16 MByte of on-board memory while natural flame images are captured on SVHS tape using a second gated intensified array camera. Digital delay generators control the timing of the firing of the laser, camera gate(s), data acquisition hardware and if applicable, the initiation of the combustion process. As shown in Fig. 1, we have examined a variety of combustion processes such as premixed and diffusion flames[6], turbulent flames[16] and fiber-supported burning droplets.[10,12]

Characterization/Applications of LII

We have tested the dependence of the LII signal upon f_v , both within a flame[6] and in the post-flame gases well above the flame.[16] In-situ tests were performed in a premixed rich flame of ethylene/air supported on a McKenna burner. A flat steel plate above the burner stabilized the flame. As the C/O ratio varies from 0.76 to 0.9, f_v changes by over an order of magnitude. At each of two detection wavelengths, 425 and 550 nm, excellent agreement between the LII signal and f_v , previously determined by line-of-sight extinction was observed as illustrated in Fig. 2. The dependence of the LII signal upon f_v in post-flame gases was performed in a chimney placed on the McKenna burner burning a rich mixture of C₂H₂/air. The chimney consisted of a meter-long steel tube with a pyrex top consisting of four side ports for optical access. Addition of N₂ to the post-flame gases in a tangential direction created a swirling action while a tripper plate within the chimney inhibited direct flow, thus homogenizing the soot containing post-flame gases. Through the technique of gravimetric sampling, f_v 's from 0.035 to 1.5 ppm were measured, produced by varying the C/O ratio from 1.53 to 2.49. As before, the linearity between the LII signal and f_v , determined through gravimetric sampling of the N₂ diluted post-flame gases is shown in Fig. 3 at each of two detected wavelengths of 450 and 550 nm. The excellent linearity between the LII signal and f_v within and outside of a flame greatly simplifies interpretation of LII images with regions of high intensity corresponding to regions of high f_v , while regions of low intensity correspond to regions of low f_v .

Demonstration of the geometric versatility of LII was performed in an ethylene/air diffusion flame surrounded by an air coflow as described in reference 6. Figure 4a is an LII image of f_v obtained with the laser sheet oriented vertically. Figures 4b-d show a sequence of LII images obtained at heights of 16.9, 14.1 and 10.0 millimeters above the burner, respectively in which the laser sheet was oriented in a horizontal plane with the LII image collected by means of a mirror placed above the non-smoking diffusion flame. The thin peripheral region containing soot is typical of laminar diffusion flames with soot converging toward the central axis at higher positions within the flame as illustrated in Fig. 4a.

As illustration of the spatial and temporal capabilities of LII, Fig. 5 shows single laser shot LII images of the soot field within the chimney illustrating the instantaneous spatial and temporal variations. Although N₂ is added to the post-flame gases to achieve mixing and uniformity of f_v , fluctuations still occur. Such characterization of the gravimetric device for different N₂ addition rates and C/O ratios of the flame was readily performed by LII.

Such images reveal several capabilities of LII as a diagnostic technique for measuring f_v . First, only with the temporal and spatial resolution capabilities of LII could such nonuniformities be observed and quantified in real time without the need for deconvolution techniques. Second, the soot within the chimney is well-removed from the flame environment and illustrates the capability of LII to reveal regions of 'cold soot' (the temperature within the pyrex top was roughly 430 K) which would not be discernable via an emission measurement, thus being complementary to that technique.

Laser-induced incandescence (LII) is ideally suited for obtaining high temporally and spatially resolved measurements of soot volume fraction in transient combustion phenomena. To further demonstrate and test the spatial and temporal capabilities of LII, f_v 's were determined within a turbulent ethylene/air diffusion flame. With identical laser intensities and detection optics, the LII signal from a $Re = 5000$ flame was calibrated via comparison to the LII signal from the chimney described above. The image in Fig. 6a is a single laser-shot beginning at 14.5 cm above the nozzle with Fig. 6b a contour plot of the LII image, the contours representing f_v in ppm. Noteworthy about this calibration method is the elimination of uncertainties in soot optical properties in the calibration of the LII signal.

Droplet combustion, with its associated small spatial scales and transient nature, typifies difficulties associated with line-of-sight extinction measurements for f_v . Natural flame luminosity, a path-integrated quantity, dominated by oxidizing soot, does not reveal the spatial distribution of soot within a flame nor f_v . Figure 7 illustrates the differences between the natural flame luminosity and LII images (Fig. 7b and 7d) for both decane and 1-chloroheptane. Image pairs 7a, 7b and 7c, 7d were each obtained approximately 2.5 seconds after ignition. Superimposed on each LII image is a picture of a ruler placed in the LII object plane prior to flame measurements. The LII image of decane, while being similar in appearance to the corresponding natural flame image, clearly reveals the soot as being concentrated in a conical region centered above the burning fuel droplet. This spatial distribution of the soot above the droplet is obscured in the natural flame image of Fig. 7a. The closed tip nature of the decane flame is also evident in Fig 7b; no soot was ever found via LII in a location above the closed tip. The LII image of 1-chloroheptane (Fig. 7d) starkly differs from the corresponding natural flame image (Fig. 7c). While both the natural flame and LII images reveal an open tipped flame, the LII image illustrates the extent of soot escape through the flame. This soot emission was easily visible by eye and some of the soot coated the optical fiber supporting the droplet. For highly sooting fuels such as monochlorinated alkanes, the natural convective flow enhances the soot emission by transporting the flame by radiative emission occurs thus opening the flame tip and allowing soot escape.[15]

These LII images of decane and chloroheptane clearly reveal the spatial and temporal capabilities of LII in measuring f_v . We have performed LII measurements on a variety of fuels to measure their relative sooting tendencies. Figure 7d further demonstrates the potential for delineating regions of cold or nonoxidizing soot by LII. Comparison between the LII and natural flame images shows the LII signal to be free from emission from excited state flame species such as C_2 , CH and OH, and can provide information complementary to chemiluminescence measurements.

Other Applications

Through the use of pulsed lasers, beam-controlling optics, and time-gated detection, LII possesses high spatial and temporal resolution in both point and planar measurements in a variety of applications. Other potential applications of LII include measurement of f_v within engine exhaust or in other pollution control situations. Other manufacturing processes require knowing the carbon content of an aerosol independently of PAH content such as in the manufacture of carbon black or carbon fibers. These applications are ideal in that detection methods as simple as photodiodes or ordinary video cameras could be used since rejection of natural flame luminosity in these applications is not an issue. Since 'point' measurements are often sufficient to characterize a reaction process or relative concentration versus time, data collection and systems need not be elaborate. Other applications of LII potentially include measurement of f_v of aerosols other than soot.

Future Plans

We are presently completing a series of detailed spectral and temporal characterization measurements of LII using different excitation wavelengths, intensities and alternative signal detection methods in order to optimize strategies for excitation and signal collection. Laser-induced spectral interferences may have little relation to f_v . Excitation intensities must also be appropriately chosen, as low intensities may not uniformly heat the soot while high intensities may result in photochemical interferences and in significant changes in the soot morphology.[17]

Our goal is to support this diagnostic technique aboard the reduced-gravity aircraft of NASA-Lewis. Both the pulsed laser system and gated intensified array camera will be compatible with a reduced-gravity environment. Plans for an aircraft rig supporting the laser and a variety of combustion experiments will be formulated this coming year. Selected laboratory measurements will identify optimal LII strategies and flame systems best suited to this reduced-gravity environment.

Acknowledgements

This program is funded through the Advanced Technology Development Program of the Microgravity Sciences and Development Program of NASA. RVW acknowledges support through contract no. NAS327-186. The official starting date for this project was Sept. 1993.

References

1. Eckbreth, A.C. J. Appl. Phys., 48:4473-4483, (1977).
2. Dasch, C.J. Appl Opt., 23:2209-2215 (1984).
3. Melton, L.A. Appl. Opt., 23:2201-2208 (1984).
4. Tait, N.A. and Greenhalgh, D.A. Proceedings of the "Optical Methods and Data Processing in Heat Transfer and Fluid Flow", Conference, London, April, (1992).
5. Hofeldt, D. L. SAE Technical Paper 930079, International Congress and Exposition, San Francisco, California, Feb.-March, (1993).
6. Vander Wal, R.L. and Weiland, K.J., J. Appl. Phys. B, in press, (1994).
7. Quay, B., Lee, T.W., Ni, T. and Santoro, R.J., Comb. and Flame 97:384-396, (1994).
8. Shaddix, C.R., Harrington, J.E. and Smyth, K.C., Twenty-Fifth Symposium (Int'l) on Combustion, The Combustion Institute, in press, (1994).
9. Cignoli, F., Benecchi, S. and Zizak, G., Appl. Opt. 33:5778-5782 (1994).
10. Vander Wal, R.L. and Dietrich, D. J., Appl. Opt., 34:1103-1107 (1994).
11. Gupta, S.B., Ni, T. and Santoro, R.J., "Spatial and Time Resolved Soot Volume Fraction Measurements in Methanol/Toluene Droplet Flames", Presented at the Technical Meeting of the Eastern States Section of the Combustion Institute, Clearwater Beach, FL, (1994).
12. Vander Wal, R.L., Dietrich, D.L. and Choi, M.Y., "Relative Soot Volume Fraction in Droplet Combustion via Laser-Induced-Incandescence", Presented at the Technical Meeting of the Eastern States Section of the Combustion Institute, Clearwater Beach, FL, (1994).
13. Dec, J. E., zur Loye, A. O., Siebers, D. L., SAE Technical Paper 910224, International Congress and Exposition, Detroit, Michigan, Feb.-March, (1991).
14. Pinson, J. A., Mitchell, D. L., Santoro, R. J. and Litzinger, T. A., SAE Technical Paper 932650, Fuels and Lubricants Meeting, Philadelphia PA, Sept. 18-21, (1993).
15. Randolph, A.L. and Law, C.K., Comb. and Flame, 64:267-284 (1986).
16. Vander Wal, R.L., Zhou, Z. and Choi, M.Y., "Laser-Induced Incandescence Calibration via Gravimetric Sampling", Presented at the Technical Meeting of the Central/Western States and Mexican Section of the Combustion Institute, San Antonio, TX, (1995).
17. Vander Wal, R.L., Choi, M.Y. and Lee, K.O., "The Effects of Rapid Heating of Soot: Implications When Using Laser-Induced-Incandescence for Soot Diagnostics", Comb. and Flame, submitted, (1994).

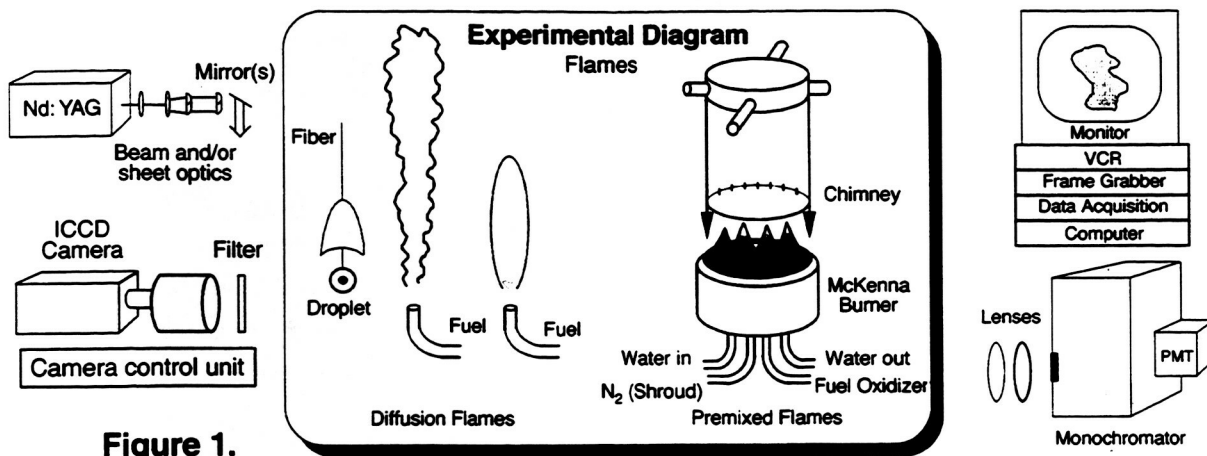


Figure 1.

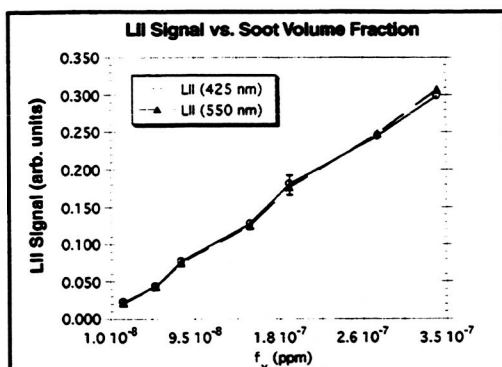


Figure 2.

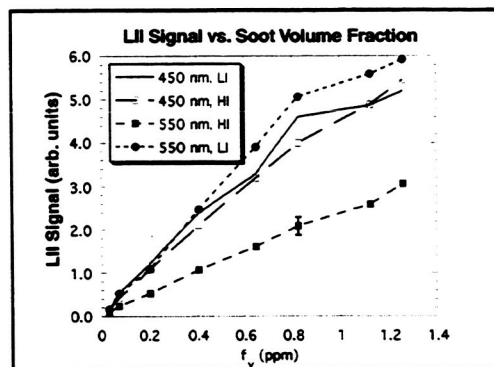


Figure 3.

Figure 2. Dependence of LII signal upon f_v within the flame using an excitation intensity of $\sim 1 \times 10^8 \text{ W/cm}^2$ with the signal detection at 425 and 550 nm. A spectral detection bandpass of 1 nm was used.

Figure 3. Dependence of LII signal upon f_v at laser intensities of 2.9×10^7 (LI) and $5.7 \times 10^7 \text{ W/cm}^2$ (HI) with detection at wavelengths 450 and 550 nm using a 1 nm spectral detection bandpass.

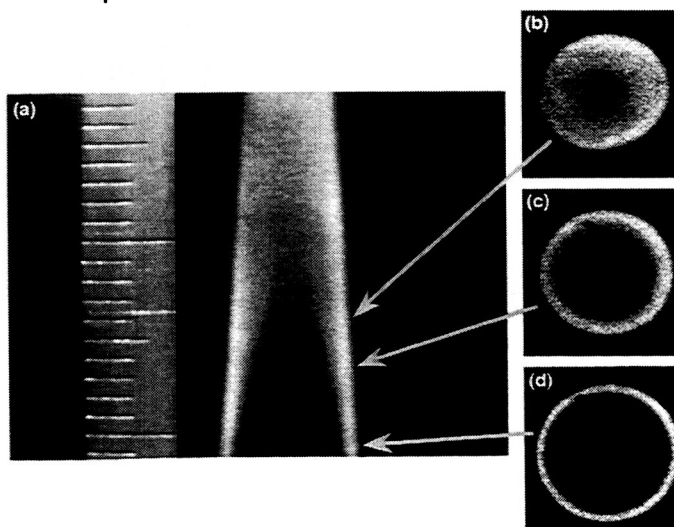


Figure 4. LII images of an ethylene diffusion flame surrounded by an air coflow. Fig. 4a was obtained with the laser sheet oriented vertically, while Fig. 4b-4d were obtained with the laser sheet oriented horizontally at heights of 10, 14.1, and 16.9 mm above the burner at the positions indicated by the arrows on Figure 4a.

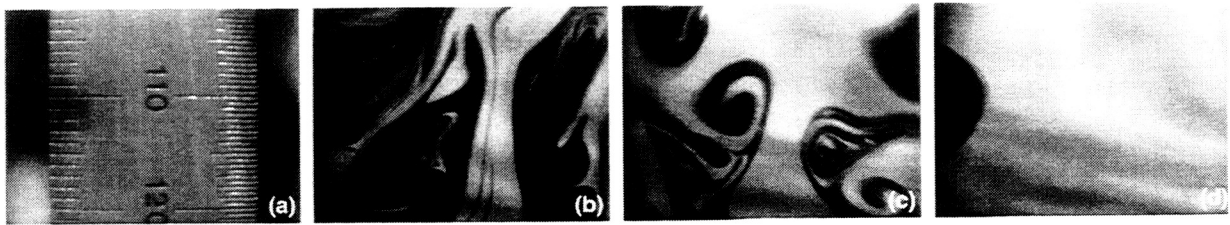


Figure 5. Spatially resolved single laser-shot LII images of the soot field within the chimney placed on the McKenna burner (5b-5d). Fig. 5a shows the ruler placed in the LII image plane prior to the measurements with the left axis markings in millimeters.

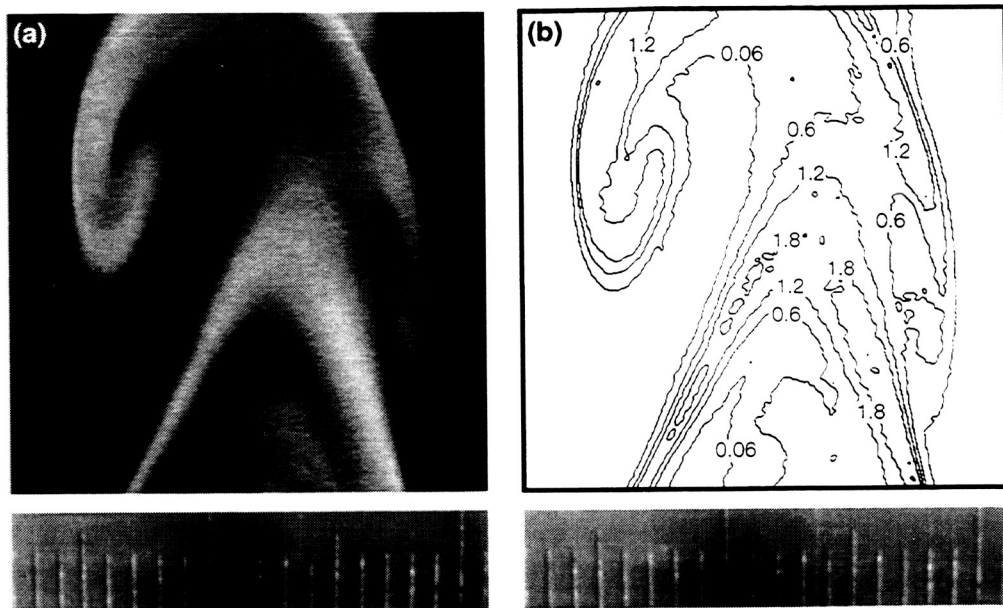


Figure 6. LII image of the $Re=5000$ turbulent gas-jet diffusion flame with the lower edge starting at 14.5 mm above the nozzle (Fig. 6a). The ruler tick marks are in millimeters. Fig. 6b is a contour plot of Fig. 6a giving f_V in ppm, determined as described in the text.

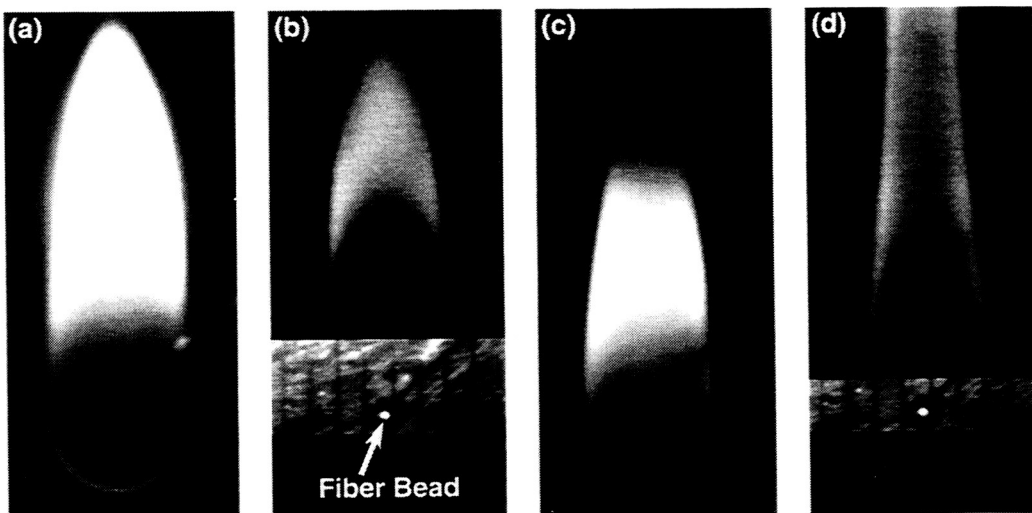


Figure 7. Simultaneous natural flame luminosity and LII images of decane (Fig. 7a-7b) and chloroheptane (Fig. 7c-7d) each obtained ~ 2.5 seconds after ignition. See text for details.